

Prospects of Pumping Power Improvements in Solid-State Lasers

Hind A. Jawad¹, Mohammed J. AbdulRazzaq^{1*}, and Khalid S. Shibib¹

¹Laser and Optoelectronics Engineering Dept, University of Technology- Iraq, Baghdad, Iraq

ABSTRACT

When the laser medium is pumped by a high pump power beam, the thermal effects are unavoidable. At this point, the gradient temperature generated inside the laser medium is essential for the simulation of the heat-induced laser medium damage. Based on experimental operating conditions listed in works of literature, a theoretical model was derived to reduce damages in solid-state lasers rod with double end-pumping geometry. Analytical thermal stress expression is obtained for the Super-Gaussian pumping profile with various exponent factors (n) and various pumping ratios (r_p). The obtained results show that the generated thermal stresses within the laser medium can be significantly reduced with the increase of both (n) and (r_p), due to more uniform distributions, and hence the prospect for pumping power scaling can be improved. Also the proposed analysis was examined and the total maximum pump power of 120 W under lasing and 90 W under the non-lasing operations, were obtained respectively at an exponent factor of ($n=32$) with a pump ratio of 1/2.

Keywords: End-pumping lasers, fracture stress, solid-state lasers, super-Gaussian pumping, thermal stress

1. INTRODUCTION

Many applications require high-power lasers. However, as the pump power increased, an uneven temperature and stress gradient will be generated in the laser rod [1]. Hence, the thermal effects (thermal birefringence, thermal lensing, and fracture due to thermally induced stress) took place and play a significant role in the design of solid-state lasers since they are inescapable [2].

Many literature works study thermal problems effects in solid-state lasers utilizing several design configurations [3–11]. A Full temperature analysis was evaluated in end-pumped solid-state lasers [12], utilizing different pumping profile types. An investigations of the heat generations in single and dual end-pumping geometries were examined numerically by [13,14] for a commonly used lasers media. By considering temperature-dependent thermal conductivity, thermal model in a double-end pumping cylindrical laser rod was fully analysis utilizing top-hat pumping and Gaussian beam profiles by [15-17].

In this work, our previous analysis of temperature distributions [18] was extended to derive a theoretical model to reduce damage stress in double-end-pumped solid-state laser rod using a Super-Gaussian pumping profile. By considering different pumping ratios, the prospect of pumping power scaling can be improved before the rod is subjected to fracture.

* mohammed.j.abdulrazzaq@uotechnology.edu.iq

2. THERMAL STRESS ANALYSIS

According to figure 1, a pump beam with an equal radius and different exponent factor (n) was focused on the center of each laser rod face to achieve a double-end-pumping configuration. By considering thermal conductivity as function of temperature, the conduction heat equation was solved analytically to estimate radial temperature distributions using Kirchoff's transform.

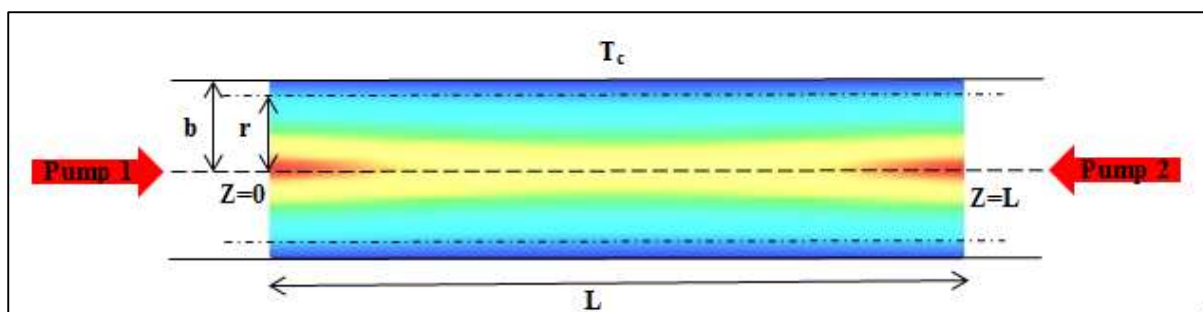


Figure 1. End-pumped geometry, where the source (Pump₁) located at $r = 0$ and (Pump₂) at $z = L$.

In general, heat equation in steady-state for a cylindrical rod with temperature-dependent-thermal conductivity can be given as [2]:

$$\nabla \cdot [K(T)\nabla T(r, z)] + Q(r, z) = 0 \quad (1)$$

where $Q(r, z)$ denotes the dissipation of heat density and $K(T)$ is the temperature-dependent thermal conductivity.

Referring to Figure1, and to establish the temperature distribution, we assume that the rod end faces are in thermal isolation while the rod length is in convection so; the boundary conditions can be written as:

$$-\frac{dU_{\text{pump}}}{dr} \Big|_{r=0} = 0 \quad (2)$$

$$-\frac{dU_{\text{unpump}}}{dr} \Big|_{r=b} = h [T_{2r=b} - T_c] \quad (3)$$

and,

$$\frac{dT_{\text{pump}}}{dr} \Big|_{r=2w} = \frac{dT_{\text{unpump}}}{dr} \Big|_{r=2w} \quad (4)$$

Therefore, two solutions might be obtained for equ.(1), one for the pump region where ($0 \leq r \leq w$) and the other for the un-pumped region where ($w < r \leq b$). Accordingly, the difference in temperature between the center and the rod edge is:

$$\Delta T_{(r,z)} = \left\{ \frac{2^{\frac{2}{n}-1} n}{r \left(\frac{2}{n}\right)} \frac{\eta h \alpha (m+1) T_0^m P}{4\pi K_0 w^2} \left[(e^{-\alpha z} + e^{-\alpha(L-z)}) \left(b^2 {}_2F_2 \left(\frac{2}{n}, \frac{2}{n}; 1 + \frac{2}{n}, 1 + \frac{2}{n}; \frac{-2b^n}{w^n} \right) - r^2 {}_2F_2 \left(\frac{2}{n}, \frac{2}{n}; 1 + \frac{2}{n}, 1 + \frac{2}{n}; \frac{-2r^n}{w^n} \right) \right) \right] \right\}^{\frac{1}{m+1}} \quad (5)$$

Now, due to temperature gradient, the rod is under stress and the fracture will occur when the maximum hoop (tangential) stress at the rod surface surpasses the tensile limits which are equal to 137.8 MPa for Nd:YAG crystal [19-22].

The formulae for the tangential stress component is given by[23]:

$$\sigma = \frac{\alpha_T E}{1-\nu} \left(\frac{1}{b^2} \int_0^b \Delta T r dr + \frac{1}{w^2} \int_0^w \Delta T r dr - \Delta T \right) \quad (6)$$

where σ is the hoop (tangential) stress component.

For a Gaussian Pumping (i.e. n=2), the hoop stress could be written as:

$$\sigma = \frac{\eta_h \alpha_T E \alpha P}{4\pi K_0 (1-\nu)} \left(E_1 \left(2 \frac{b^4}{w^4} \right) + \ln \left(\frac{b^4}{w^4} \right) + \frac{w^2}{2b^2} \left(e^{-\frac{2b^2}{w^2}} - 1 \right) + \frac{1}{2} \left(\frac{1}{e^2} - 1 \right) - 3 \right) \quad (7)$$

While, for a Super-Gaussian pumping (i.e. n=4), the hoop stress is:

$$\sigma = \frac{\eta_h \alpha_T E \alpha P}{8\pi K_0 (1-\nu) 2^{\frac{2}{3}}} \left(1 + E_1 \left(2 \frac{b^4}{w^4} \right) + \ln \left(\frac{b^4}{w^4} \right) - E_1(2) + \sqrt{\frac{\pi}{2}} \left(\frac{w^2}{b^2} \operatorname{erfi} \left(\frac{\sqrt{-2} b^2}{w^2} \right) + \operatorname{erfi}(\sqrt{-2}) \right) \right) \quad (8)$$

for n=6

$$\sigma = \frac{\eta_h \alpha_T E \alpha P}{9\pi K_0 (1-\nu) 2^{\frac{2}{3}}} \left(\frac{9}{2} + E_1 \left(2 \frac{b^6}{w^6} \right) - \frac{1}{2} \left(\ln \left(\frac{b^6}{w^6} \right) + E_1 \left(2 \frac{b^6}{w^6} \right) + E_1(2) \right) - \frac{2^{\frac{2}{3}}}{4} \left(\frac{\Gamma \left(\frac{1}{3}, -\frac{2b^6}{w^6} \right)}{\sqrt[3]{-b^6}} + \frac{\Gamma \left(\frac{1}{3}, -2 \right)}{\sqrt[3]{-1}} \right) \right) \quad (9)$$

for n=16

$$\sigma = \frac{\eta_h \alpha_T E \alpha P}{32\pi K_0 (1-\nu) 2^{\frac{7}{8}}} \left(8 - E_1(2) + E_1 \left(2 \frac{b^{16}}{w^{16}} \right) - \frac{1}{2} \ln \left(\frac{b^{16}}{w^{16}} \right) - \frac{2^{\frac{7}{8}}}{4} \left(\frac{\Gamma \left(\frac{1}{8}, -\frac{2b^{16}}{w^{16}} \right)}{\sqrt[8]{-b^{16}}} + \frac{\Gamma \left(\frac{1}{8}, -2 \right)}{\sqrt[8]{-1}} \right) \right) \quad (10)$$

and for n=32

$$\sigma = \frac{\eta_h \alpha_T E \alpha P}{128\pi K_0 (1-\nu) 2^{\frac{15}{8}}} \left(16 - E_1(2) + E_1 \left(2 \frac{b^{32}}{w^{32}} \right) - \frac{1}{2} \ln \left(\frac{b^{32}}{w^{32}} \right) - \frac{2^{\frac{15}{8}}}{2} \left(\frac{\Gamma \left(\frac{1}{16}, -\frac{2b^{32}}{w^{32}} \right)}{\sqrt[16]{-b^{32}}} + \frac{\Gamma \left(\frac{1}{16}, -2 \right)}{\sqrt[16]{-1}} \right) \right) \quad (11)$$

3. RESULTS AND DISCUSSION

Before evaluating the fractural thermal stress, we make a comparison with an earlier numerical analysis presented by [24] to examine our proposed model and a good agreement was obtained as listed in Table 1.

It is clear that the exponent factor has a significant impact on the temperature distributions. Hence, the temperature distributions were found to be maximum for a Gaussian pumping (n=2), and then decreased for a Super-Gaussian profiles as the temperature distribution tends to be more uniform as can be seen in Table 1.

Table 1 Comparison between the proposed model and a numerical work

Beam profile	Maximum Temperature Difference (K)		
	Proposed Model	Numerical Analysis [24]	% error
Gaussian (n=2)	372	374.4	0.64
n=4	374.871	373.765	0.29
n=6	373.333	372.652	0.18
n=10	370.795	371.761	0.26
n=30	369.743	368.421	0.35

Figure 2 depicts the temperature gradient of double end Super-Gaussian pumping with different exponent factors (n).

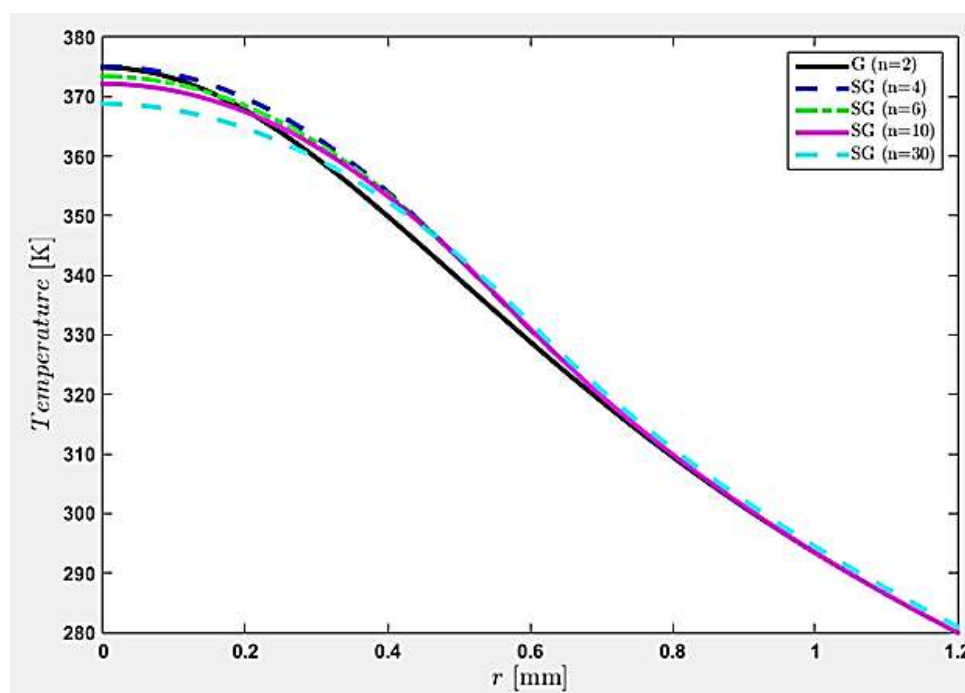


Figure 2. Temperature gradient of double end super-Gaussian pumping with different exponent factors (n).

It is clear that, the maximum temperature difference is about 372 K and decreased exponentially along the rod radius due to intensive absorption power. According to these results, Figure 2 shows an excellent matching with the same parameters used for a previous earlier work listed by [24].

Now, according to these results with the help of input parameters mentioned in Table 2, we try to calculate the maximum input power that the laser rod can be handled before the fracture occurs. By solving Eq. (6), the maximum hoop stress was calculated under the lasing operation (i.e. $\eta_h = 32\%$) utilizing different spot to rod radius, namely pumping ratios (r_p) as (1/4, 1/3, and 1/2), respectively as shown in Figure 3 (a, b, and c).

Table 2 Input Laser Parameters.

Poisson's ratio (ν)	0.25
Fractional heat loading (η_h)	32% and 43%
Laser rod radius (b)	1.2 mm
Laser rod length (L)	4 mm
Absorption coefficient (α)	350 m ⁻¹
Thermal conductivity (K_0)	13 W.m ⁻¹ .K ⁻¹
Temperature (T_0)	164.17 K
Cooling temperature (T_c)	300 K
Power coefficient of thermal conductivity (m)	-0.75
Heat-transfer coefficient (h)	0.02 W.mm ⁻² .K ⁻¹
Young modulus (E)	310 GPa
Pump radius (w)	0.3 mm

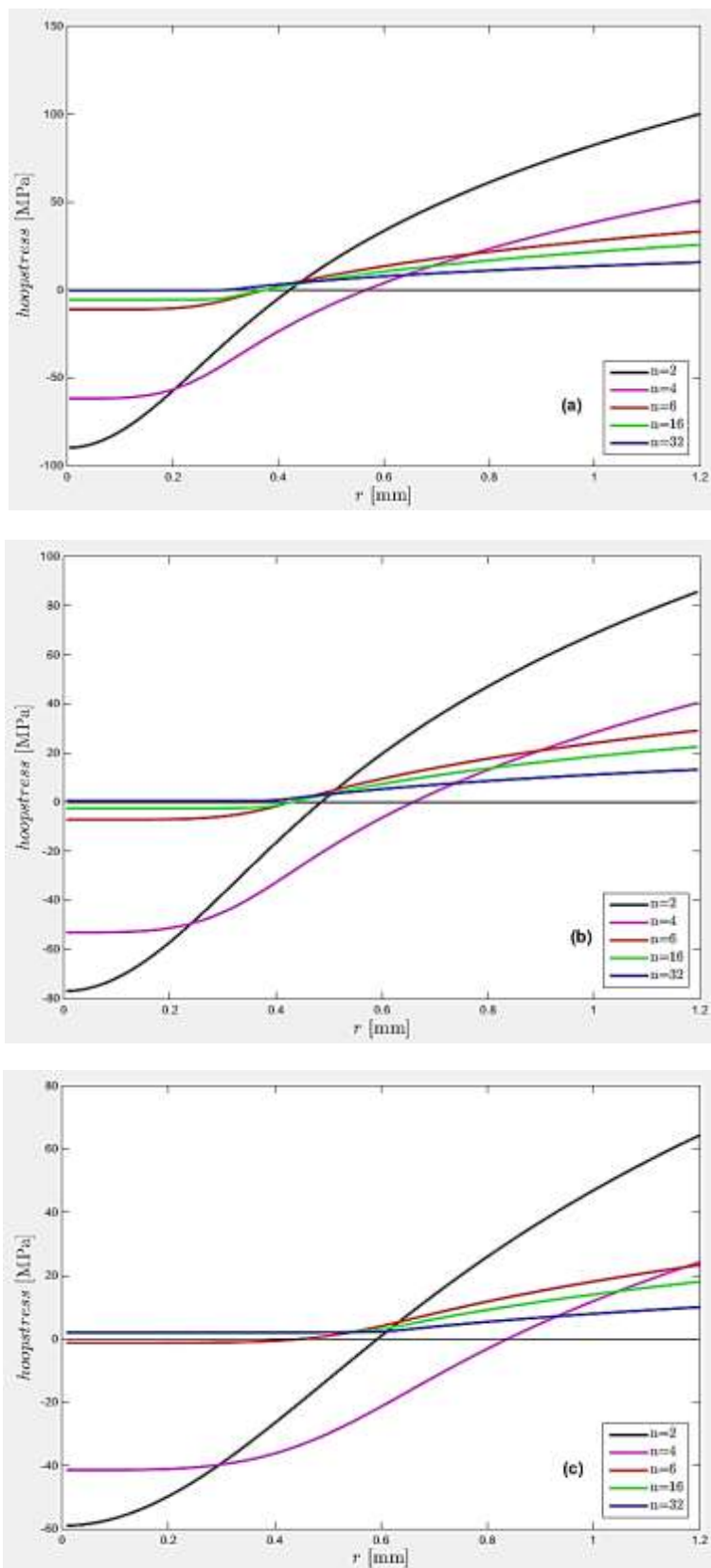


Figure 3. Maximum hoop stresses under lasing operation ($\eta_h=32\%$) with different exponent factors for (a) $r_P = 1/4$, (b) $r_P = 1/3$, and (c) $r_P = 1/2$.

Under the non-lasing operation (i.e. $\eta_h = 43\%$), the maximum hoop stress was calculated utilizing the same pumping ratio as shown in figure 4 (a,b, and c).

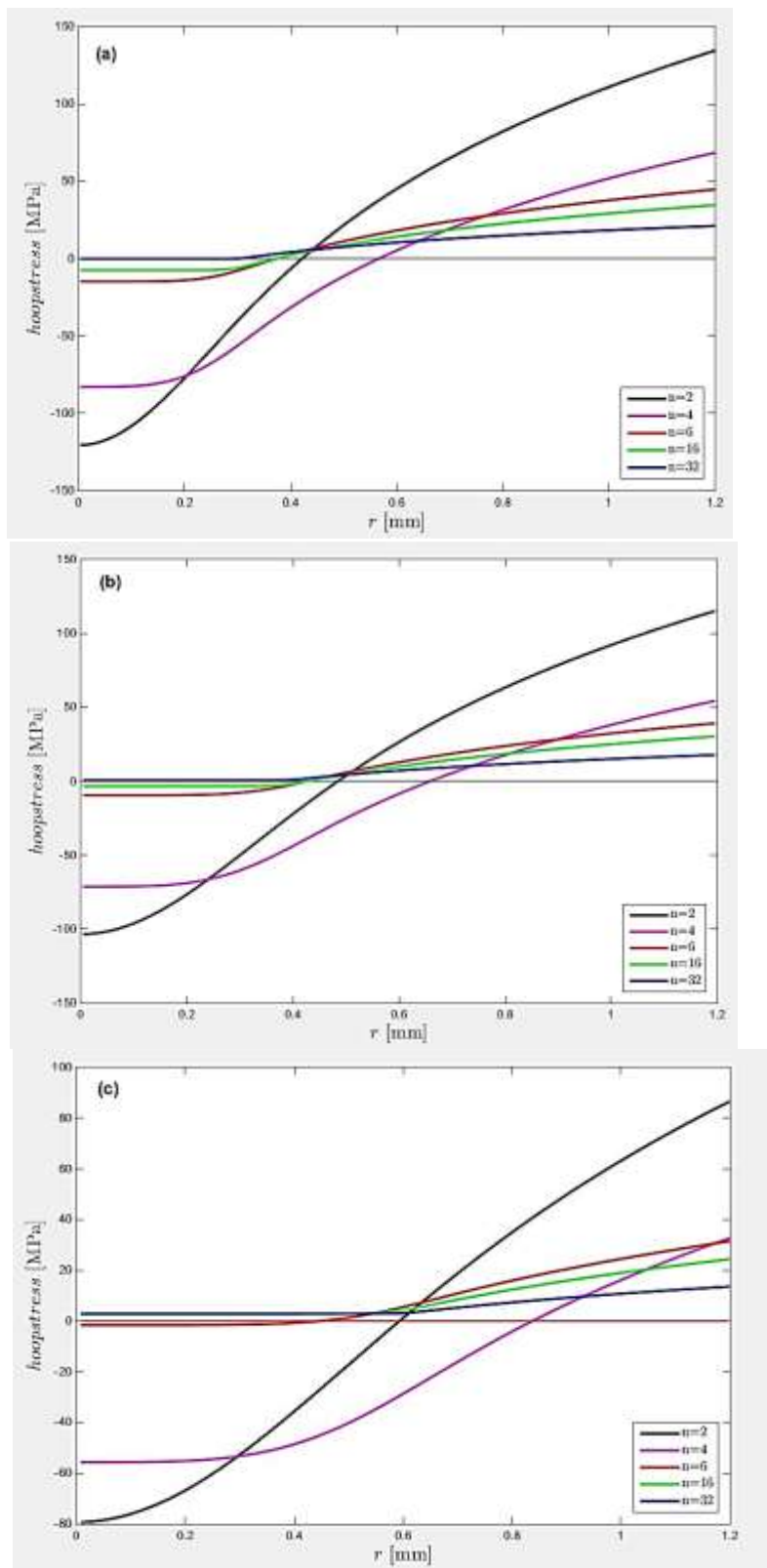


Figure 4. Maximum hoop stresses under the non-lasing operation ($\eta_h=43\%$) with different exponent factors for (a) $r_p = 1/4$, (b) $r_p = 1/3$, and (c) $r_p = 1/2$.

In both cases, the obtained results show that as the exponent factor increased; the maximum hoop stress decreased obviously and the prospect for pumping power scaling can be improved before the fracture occurred as mentioned in table 3. However, under the lasing operation, the stresses were much lower as compared to non-lasing operation and hence the maximum pumping power on each face of the rod was 60 W before a fracture occurs at an r_p of (1/2).

Table 3 Maximum handling powers (with and without lasing) for different exponent factors and pumping ratios

Exponent factor	Total Pump Power (W)									
	Lasing Operation					Non-lasing Operation				
	n=2	n=4	n=6	n=16	n=32	n=2	n=4	n=6	n=16	n=32
$r_p = 1/4$	12	23	25	48	76	9	17	22	35	56
$r_p = 1/3$	14	28	32	54	90	10	21	26	40	66
$r_p = 1/2$	19	35	45	68	120	14	26	34	52	90

4. CONCLUSIONS

This work presents a solution of fracture limit in solid-state lasers by solving conduction heat equation analytically using Kirchhoff's transform method. With the help of super-Gaussian pumping profile, the temperature distributions and the maximum hoop stress were evaluated in double-end-pumped configuration. The obtained results show that as the exponent factor increased, the maximum hoop stress decreased and the pumping power can be improved before the fracture occurs. According to the used parameters under the lasing operation, the maximum pumping power was 120 W with a pumping ratio (r_p) of 1/2.

REFERENCES

- [1] K. Yumashev and P. Loiko, Thermal stress and end-bulging in monoclinic crystals: the case study of double tungstates, *Appl. Opt.*, vol. 56, no. 13, pp. 3857–3866, 2017.
- [2] W. Xie, Siu-Chung Tam, Yee-Loy Lam, Hongru Yang, Jingang Liu, Jianhui Gu, Wilson Tan., Thermal and optical properties of diode side-pumped solid state laser rods, *Opt. Laser Technol.*, vol. 32, no. 3, pp. 193–198, 2000, doi: 10.1016/S0030-3992(00)00042-6.
- [3] B. Fang, H. Zhulong, L. Jingliang, C. Xinyu, W. Chunting, and J. Guangyong, Thermal analysis of double-end-pumped Tm:YLF laser, *Laser Phys.*, vol. 25, no. 7, p. 75003, 2015, doi: 10.1088/1054-660X/25/7/075003.
- [4] S. Elahi, P. and Morshedi, And Thermo-Optical EffectS In Double-End-Pumped Slab Laser, *J. Eng. Phys. Thermophys.*, vol. 84, no. 6, pp. 1142–1147, 2011.
- [5] B. A. Usievich, V. A. Sychugov, F. Pigeon, and A. Tishchenko, Analytical treatment of the thermal problem in axially pumped solid-state lasers, *IEEE J. Quantum Electron.*, vol. 37, no. 9, pp. 1210–1214, 2001, doi: 10.1109/3.945327.
- [6] F. Kalantarifard, H. Nadgaran, and P. Elahi, The analytical and numerical investigation of thermo-optic effects in double-end-pumped solid state lasers, *Int. J. Phys. Sci.*, vol. 4, no. 6, pp. 385–389, 2009.
- [7] W. Xie, Y. K. Kwon, W. Hu, and F. Zhou, Thermal modeling of solid state lasers with super-Gaussian pumping profiles, *Opt. Eng.*, vol. 42, no. 6, pp. 1787–1794, 2003.
- [8] M. Mojahedi and H. Shekoohejad, Thermal Stress Analysis of a Continuous and Pulsed End-Pumped Nd:YAG Rod Crystal Using Non-Classic Conduction Heat Transfer Theory, *Brazilian J. Phys.*, vol. 48, no. 1, pp. 46–60, 2018, doi: 10.1007/s13538-017-0538-4.
- [9] Y. Wen, N. Liu, Z. Fan, C. Wu, and G. Jin, Pulsed laser diode dual-end pumped double-end

- bonded Tm : YAG transient thermal effect analysis Pulsed laser diode dual-end pumped double-end bonded Tm : YAG transient thermal effect analysis, pp. 1–7, 2019, doi: 10.1088/1742-6596/1237/2/022190.
- [10] M. Y. Ghadban, K. S. Shibib, and M. J. Abdulrazzaq, Analytical model of transient thermal effects in microchip laser crystal, *AIP Conf. Proc.*, vol. 2213, no. March, 2020, doi: 10.1063/5.0000277.
- [11] C. Xinyu, L. Jingliang, W. Chunting, W. Ruiming, and J. Guangyong, Thermal Effects Analysis of High-Power Slab Tm:YLF Laser with Dual-End-Pumped Based on COMSOL Multiphysics, *Integr. Ferroelectr.*, vol. 210, no. 1, pp. 197–205, 2020, doi: 10.1080/10584587.2020.1728823.
- [12] L. Cini and J. I. Mackenzie, Analytical thermal model for end-pumped solid-state lasers, *Appl. Phys. B Lasers Opt.*, vol. 123, no. 12, 2017, doi: 10.1007/s00340-017-6848-y.
- [13] M. Sayem El-Daher, Finite element analysis of thermal effects in diode end-pumped solid-state lasers, *Adv. Opt. Technol.*, vol. 2017, 2017, doi: 10.1155/2017/9256053.
- [14] R. M. El-Agmy and N. Al-Hosiny, Thermal analysis and experimental study of end-pumped Nd: YLF laser at 1053 nm, *Photonic Sensors*, vol. 7, no. 4, pp. 329–335, 2017, doi: 10.1007/s13320-017-0412-6.
- [15] M. J. AbdulRazzaq, A. Z. Mohammed, A. K. Abass, and K. S. Shibib, A new approach to evaluate temperature distribution and stress fracture within solid state lasers, *Opt. Quantum Electron.*, vol. 51, no. 9, pp. 1–10, 2019, doi: 10.1007/s11082-019-2012-8.
- [16] M. J. AbdulRazzaq, K. S. Shibib, and S. I. Younis, Temperature distribution and stress analysis of end pumped lasers under Gaussian pump profile, *Opt. Quantum Electron.*, vol. 52, no. 8, pp. 1–9, 2020, doi: 10.1007/s11082-020-02499-y.
- [17] M. J. Abdulrazzaq and K. A. Hubeatir, Analysis of Thermal Effects within Cylindrical Shape Solid-State Laser Rod, vol. 1002, pp. 264–272, 2020, doi: 10.4028/www.scientific.net/MSF.1002.264.
- [18] H. A. Jawad and M. J. Abdulrazzaq, Effects of pumping profiles on the temperature distributions in double- end pumped solid-state lasers : A comparison study, vol. 40, no. July 2021, pp. 343–349, 2022.
- [19] C. Pfistner, R. Weber, H. P. Weber, S. Merazzi, and R. Gruber, Thermal beam distortions in end-pumped Nd: YAG, Nd: GSGG, and Nd: YLF rods, *IEEE J. Quantum Electron.*, vol. 30, no. 7, pp. 1605–1615, 1994.
- [20] A. K. Cousins, Temperature and Thermal Stress Scaling in Finite-Length End-Pumped Lasers Rods, *IEEE J. Quantum Electron.*, vol. 28, no. 4, pp. 1057–1069, 1992, doi: 10.1109/3.135228.
- [21] L. Yan and C. H. Lee, Thermal effects in end-pumped Nd: phosphate glasses, *J. Appl. Phys.*, vol. 75, no. 3, pp. 1286–1292, 1994.
- [22] S. Chénais, F. Balembois, F. Druon, G. Lucas-Leclin, and P. Georges, Thermal lensing in diode-pumped ytterbium lasers-Part I: theoretical analysis and wavefront measurements, *IEEE J. Quantum Electron.*, vol. 40, no. 9, pp. 1217–1234, 2004.
- [23] W. Koechner, *Solid-State Laser Engineering: Fourth Extensively Revised and Updated Edition*, Springer Ser. Opt. Sci., vol. 1, no. 1, p. ALL-ALL, 1996.
- [24] H. M. Ahmed, M. J. A. Razzaq, and A. K. Abass, Numerical thermal model of diode double-end-pumped solid state lasers, *Int. J. Nanoelectron. Mater.*, vol. 11, no. 4, pp. 473–480, 2018.

